

Phase diagram of the 3D Axial-Next-Nearest-Neighbor Ising model

A. Gendiar^{1,2} and T. Nishino¹

¹ Department of Physics, Faculty of Science, Kobe University, Kobe 657-8501, Japan

² Institute of Electrical Engineering, Slovak Academy of Sciences,

Dúbravská cesta 9, SK-842 39 Bratislava, Slovakia

(Dated: May 21, 2019)

The three-dimensional axial-next-nearest-neighbor Ising (ANNNI) model is studied by an improved tensor product variational approach (TPVA). A detailed phase diagram is constructed for the model. In contrast to the phase diagram obtained by the mean-field approximation, no *devil's staircase* structure is observed. Inside the spin modulated phase the wave vector varies continuously. A scaling exponent $\vartheta \approx \frac{1}{2}$ of the wave vector is found at the phase boundary between the ferromagnetic and the modulated phases.

PACS numbers: 64.60.Fr, 02.70.-c, 64.70.Rh, 75.10.Hk

Periodically modulated magnetic structures have attracted scientific interest for several decades both experimentally and theoretically. A non-trivial phase diagram obtained by experimental measurements in cerium antimonide (CeSb) showed a variety of different commensurately ordered magnetic structures with the underlying lattice [1]. The three-dimensional (3D) $S = \frac{1}{2}$ axial next-nearest-neighbor Ising (ANNNI) model has been considered as a theoretical candidate for CeSb since it exhibits a rich phase structure when it is treated by mean-field approximation [2]. The 3D $S = \frac{1}{2}$ ANNNI model is another example that shows a non-trivial spin modulated phase - the so-called devil's staircase - within the framework of the mean-field approximation. [3, 4, 5]. Recently, Monte Carlo simulations have been applied to the $S = \frac{1}{2}$ model with a finite number of spin layers [6]. Henkel and Pleimling considered an anisotropic scaling at the Lifshitz point using the Wolff cluster algorithm and several critical exponents have been calculated [7]. The purpose of this letter is to clarify the phase structure of the 3D $S = \frac{1}{2}$ ANNNI model with the use of a novel numerical method. We point out that there is no devil's staircase structure.

We study the ANNNI model on a simple cubic lattice with the size of $L \times \infty \times \infty$ along the X -, Y -, and Z -axis, respectively, for sufficiently large L . The model is described by the Hamiltonian

$$\mathcal{H} = -J_1 \sum_{i,j,l} \sigma_{i,j,l} (\sigma_{i+1,j,l} + \sigma_{i,j+1,l} + \sigma_{i,j,l+1}) + J_2 \sum_{i,j,l} \sigma_{i,j,l} \sigma_{i+2,j,l}, \quad (1)$$

where the subscripts i , j , and k of the $S = \frac{1}{2}$ Ising spin $\sigma = \pm 1$ refer to the axial X -, Y -, and Z - coordinates, respectively. The ferromagnetic interaction $J_1 > 0$ acts between the nearest-neighbors, and $J_2 > 0$ is the competing antiferromagnetic interaction between the next-nearest-neighbors only along the x -axis.

We analyze the model using the tensor product variational approach (TPVA) [8] which is an extension of the Kramers-Wannier approximation to the 3D models [9].

TPVA variationally maximizes the partition function per layer

$$\lambda(\Psi) = \frac{\langle \Psi | \mathcal{T} | \Psi \rangle}{\langle \Psi | \Psi \rangle}, \quad (2)$$

where the trial state $|\Psi\rangle$ for the layer-to-layer transfer matrix \mathcal{T} is constructed as a product of local variational factors. Since the ANNNI model has the next-nearest neighbor interaction, it is natural to write down the trial state in a layer as

$$\Psi = \prod_{i,j} V \begin{pmatrix} \sigma_{i,j} & \sigma_{i+1,j} & \sigma_{i+2,j} \\ \sigma_{i,j+1} & \sigma_{i+1,j+1} & \sigma_{i+2,j+1} \end{pmatrix}, \quad (3)$$

where the local variational factors V partially overlap each other. There are $2^6 = 64$ variational parameters in total for each V . In order to study non-uniform spin modulated phases we allow positional dependence on V . We use the finite system density matrix renormalization group [10, 11, 12] to calculate the numerator and the denominator in Eq. (2). The variational state $|\Psi\rangle$ is improved by means of successive improvements for each local factor. We performed the calculations up to the system size $L = 30\,000$ whereas $L = 2000$ is sufficiently large to reach the thermodynamic limit for most of the cases. After the $|\Psi\rangle$ is optimized we calculate the spontaneous magnetization per layer

$$\langle \sigma_{i,j} \rangle = \frac{\langle \Psi | \sigma_{i,j} | \Psi \rangle}{\langle \Psi | \Psi \rangle}. \quad (4)$$

TABLE I: The critical temperature T_c for the 3D Ising model ($J_2 = 0$). We calculate the relative errors ε with respect to T_c obtained by Monte Carlo simulations [13].

Numerical method	T_c	$\varepsilon/[\%]$
Mean-field approximation [4]	6.000	33.0
Kramers-Wannier approximation [9]	4.587	1.7
TPVA with 16 parameters [8]	4.570	1.3
TPVA with 64 parameters	4.554	0.9
Monte Carlo simulations	4.512	—

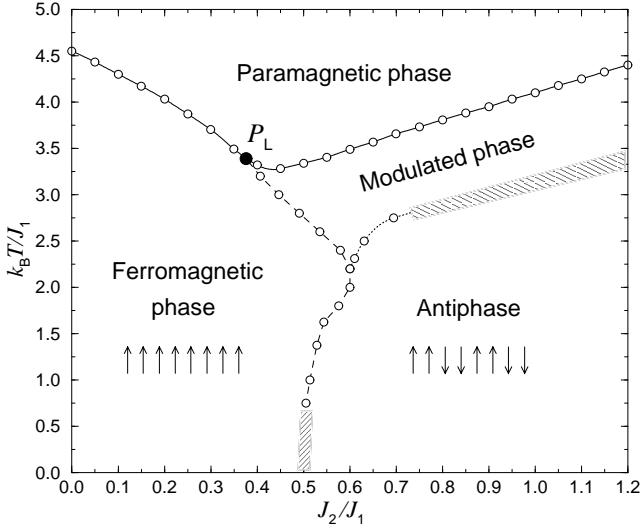


FIG. 1: The phase diagram for the 3D ANNNI model with four phases. The points represent the calculated phase boundary. In the dashed regions, the phase boundary was not determined precisely.

Since the competing interaction exists only along X -direction, the system is translationally invariant with respect to the Y - and Z -directions. Therefore, the spontaneous magnetization $\langle \sigma_{i,j} \rangle$ is independent on j and we simplify the notation as $\langle \sigma_i \rangle$ in the following.

First of all, we estimate the numerical error in TPVA with the trial state $|\Psi\rangle$ in Eq.(3). We compare the transition temperature T_c when $J_2 = 0$, i. e., the pure Ising model. Table I shows the obtained critical temperature T_c and those obtained with other numerical methods. It is obvious that the mean-field approximation overestimates T_c . TPVA with the 64 variational parameters gives better T_c than the original TPVA with 16 free parameters.

Figure 1 shows the phase diagram. In contrast to the previous mean-field calculations, the model exhibits only four phases: (1) a paramagnetic disordered phase, (2) a uniformly ordered ferromagnetic phase, (3) a modulated phase, and (4) an antiphase. The first three phases meet at the calculated Lifshitz point P_L located at $J_2^L/J_1^L=0.376$ and $k_BT_L/J_1^L=3.361$. Inside the modulated phase a wavy spin structure is observed. Figure 2 shows an example of the structure at $J_2/J_1 = 0.8$ and $k_BT/J_1 = 3.3$. The uppermost graph and the middle graph show, respectively, the small-scale ($0 < i \leq 30$) and the large-scale ($0 < i \leq 300$) spin structures for $L = 2000$ -site system ($-999 \leq i \leq 1000$).

We use the Fourier transform (FT) of the magnetization in order to obtain the wave vector k of the modulation. The lowermost graph in Fig. 2 displays the intensity

$$I_k = \left| \frac{1}{L} \sum_{n=-L/2}^{L/2-1} \langle \sigma_n \rangle e^{-ikn} \right| \quad (5)$$

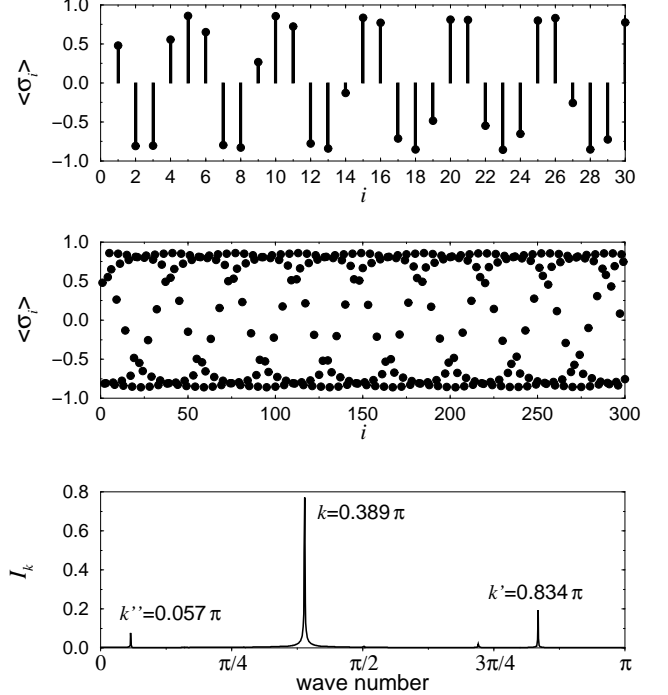


FIG. 2: The spin structure at $J_2/J_1 = 0.8$ and $k_BT/J_1 = 3.3$. The two upper graphs display the magnetization $\langle \sigma_i \rangle$. The bottom graph shows the Fourier transform of the structure above.

of the magnetization in the two upper graphs. The most dominant peak appears at $k = 0.389\pi$. The two sub-peaks at $k' = 0.834\pi \approx 2\pi - 3k$ and at $k'' = 0.057\pi \approx 2\pi - 5k$ correspond to the 3rd and the 5th higher harmonics, respectively. The presence of the higher harmonics denotes a non-linear deformation of the wave from the simple sinusoidal one [14].

The ferromagnetic phase is described by $k = 0$ and the antiphase by $k = \frac{\pi}{2}$. At the boundary between ferromagnetic and the modulated phases, the wave vector k behaves continuously [15]. The wave vector increases as J_2/J_1 grows inside the modulated phase and finally converges to $k = \frac{\pi}{2}$ in the limit $J_2/J_1 \rightarrow \infty$. In the same manner k converges to $\frac{\pi}{2}$ towards the boundary between the modulated phase and the antiphase. Towards the paramagnetic disordered phase, the magnetization of a modulated structure gradually decreases to zero in the modulated phase. *The wave vector k varies smoothly and does not lock-in at any rational (commensurate) values of low-orders.* Such a property of the modulated phase in the 3D ANNNI model contradicts the previous results carried out by the mean-field approximation, which support the stairs-like behavior.

In order to obtain a parameter dependence of the wave vector k , we perform a scaling analysis on it. Figure 3 shows the parameter line where we calculate k for the scaling analysis. The parameter line is chosen so that it passes through the whole modulated phase and intersects the phase boundary with the ferromagnetic phase.

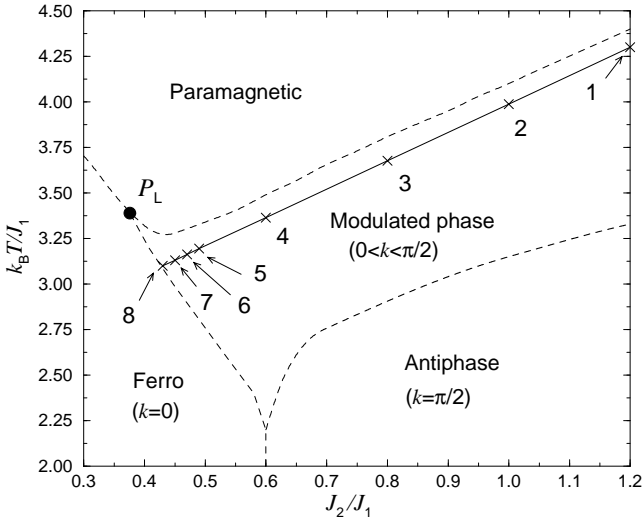


FIG. 3: The parameter line passing through the modulated phase that we used for the scaling analysis.

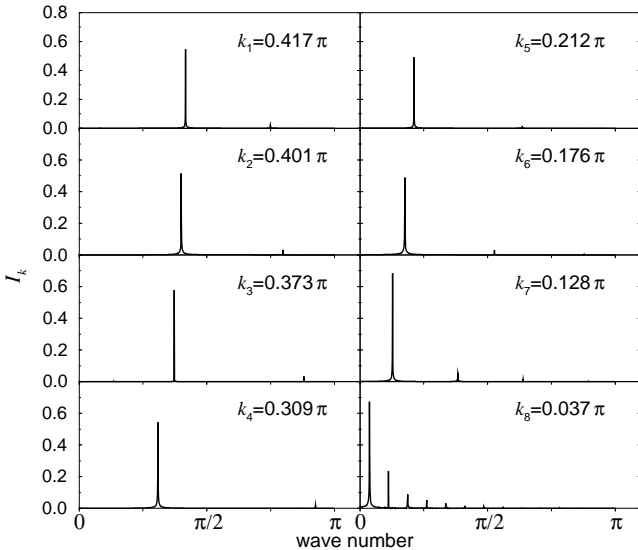


FIG. 4: The Fourier transform analysis applied to the eight points lying on the parameter line in Fig. 3.

The intersection point is located at $J_2^c/J_1^c = 0.4284$ and $k_B T_c/J_1^c = 3.0975$.

On the parameter line we select several representative points that are shown by numbers in Fig. 3. The Fourier intensities of $\langle \sigma_i \rangle$ at the selected points are presented in Fig. 4. Near the boundary with the ferromagnetic phase the waves become strongly non-sinusoidal and for this reason the intensity of the equidistantly distributed higher harmonics increases.

Let us define a distance d measured from the point of intersection to any point with the coordinates $(J_2/J_1,$

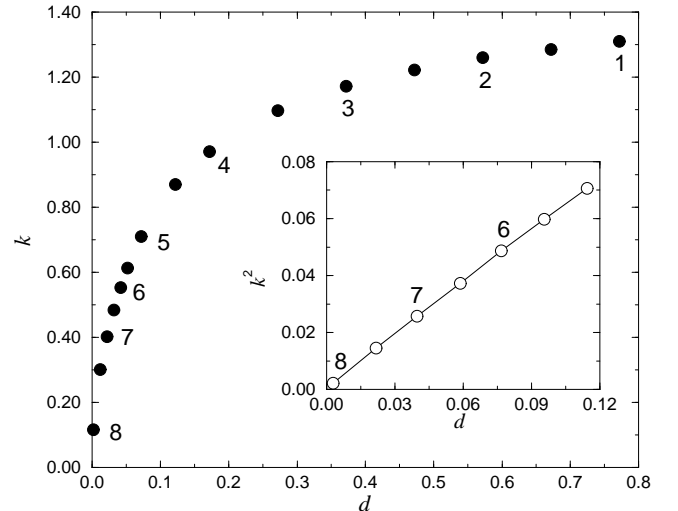


FIG. 5: Dependence of the wave vector k on the distance d . Inset: the squared wave vector versus the distance exhibits the linear behavior at a vicinity of the phase boundary.

$k_B T/J_1$) on the parameter line

$$d = \sqrt{\left(\frac{J_2^c}{J_1^c} - \frac{J_2}{J_1}\right)^2 + \left(\frac{k_B T_c}{J_1^c} - \frac{k_B T}{J_1}\right)^2}, \quad (6)$$

for the purpose of obtaining an exponent ϑ from the scaling relation

$$k \propto d^\vartheta. \quad (7)$$

In Fig. 5 we plotted the dependence of the wave vector k on the distance d . Evidently, from the behavior of k^2 shown in the inset of Fig. 5, the exponent ϑ is almost $\frac{1}{2}$. A least-square fitting for the data shown in the inset yields $\vartheta^{-1} = 2.05$. Thus it is conjectured that the phase transition between the modulated and the ferromagnetic phases in the 3D ANNNI model is classified by the critical exponent $\vartheta \approx \frac{1}{2}$.

In conclusion, we constructed the phase diagram of the 3D ANNNI model by use of TPVA. We have found that there was no devil's staircase behavior in the magnetic modulation. The scaling law for the spin modulated wave was found with the critical exponent $\vartheta \approx \frac{1}{2}$.

A. G. thank A. Šurda for an interesting discussion about the incommensurate phases in the ANNNI model. This work has been partially supported by the Grant-in-Aid for Scientific Research from Ministry of Education, Science, Sports and Culture (Grant No. 09640462 and No. 11640376) and by the Slovak Grant Agency, VEGA No. 2/7201/21. A.G. is also supported by Japan Society for the Promotion of Science (P01192).

[1] P. Fisher, B. Lebech, G. Meier, B. D. Rainford, and O. Vogt, *J. Phys. C* **11**, 345 (1978); J. Rossat-Mignod, P. Burlet, J. Villain, H. Bartholin, Wang Tcheng-Si, D. Florence, O. Vogt, *Phys. Rev. B* **16**, 440 (1977).

[2] J. von Boehm and P. Bak, *Phys. Rev. Lett.* **42**, 122 (1979).

[3] P. Bak and J. von Boehm, *Phys. Rev. B* **21**, 5297 (1980).

[4] P. Bak, *Rep. Prog. Phys.* **45**, 587 (1982).

[5] M. E. Fisher and W. Selke, *Phys. Rev. Lett.* **44**, 1502 (1980).

[6] W. Selke, M. Pleimling, and D. Catrein, *Eur. Phys. J. B* **27**, 321 (2002).

[7] M. Henkel and M. Pleimling, *Comp. Phys. Commun.* **147**, 161 (2002).

[8] T. Nishino, K. Okunishi, Y. Hieida, N. Maeshima, and Y. Akutsu, *Nucl. Phys. B* **575**, 504 (2000); T. Nishino, K. Okunishi, Y. Hieida, N. Maeshima, Y. Akutsu, and A. Gendiar, *Prog. Theor. Phys.* **105**, 409 (2001); A. Gendiar and T. Nishino, *Phys. Rev. E* **65**, 046702 (2002).

[9] H. A. Kramers and G. H. Wannier, *Phys. Rev.* **60**, 263 (1941).

[10] S. R. White, *Phys. Rev. Lett.* **69**, 2863 (1992); S. R. White *Phys. Rev. B* **48**, 10345 (1993).

[11] Originally we have formulated TPVA by use of the corner transfer matrix renormalization group [T. Nishino and K. Okunishi, *J. Phys. Soc. Jpn.* **65**, 891 (1996)]. Here we employed DMRG because the incommensurately and/or commensurately modulated phases can be easily determined by DMRG [A. Gendiar and A. Šurda, *Phys. Rev. B* **62**, 3960 (2000)].

[12] The numerical calculations were performed by MIPSpro Fortran compiler on the RISC Unix cluster and by Compaq Fortran compiler on HPC-Alpha UP21264 Linux workstations.

[13] W. Janke and R. Villanova, *Nucl. Phys. B* **489**, 679 (1997).

[14] The modulated wave is strongly non-sinusoidal at the vicinity of the ferromagnetic phase.

[15] The smallest wave vector that we actually observed is $k \approx \frac{\pi}{1000}$ for the system size $L = 30\,000$.